

Biomimetic oxidations using transition metal complexes encapsulated in zeolites

D. Srinivas and S. Sivasanker*

Catalysis Division, National Chemical Laboratory, Pune 411 008, India

An account of biomimetic oxidations by metal phthalocyanines, tri- and tetra-aza macrocycles, Schiff bases (salen and saloph), dimeric Cu-acetate and Co-Mn-acetate complexes encapsulated in zeolite-Y and molecular sieves is reported. The selective oxidation reactions investigated include epoxidation of styrene, hydroxylation of phenol, oxidation of *p*-xylene to terephthalic acid, ethylbenzene to acetophenone and cyclohexane, cyclohexanol and cyclohexanone to adipic acid. In all these reactions, the encapsulated metal complexes exhibit enhanced activity or selectivity compared to the “neat” complexes. The reasons for the enhanced activity of metal complexes upon encapsulation in zeolites are reported.

KEY WORDS: transition metal complexes; encapsulation in zeolites; zeozymes; selective oxidation; biomimetic oxidation; molecular sieves; zeolites; spectroscopic characterization; EPR.

1. Introduction

Cytochrome P450, a monooxygenase, found in almost all living organisms, catalyzes the selective oxidation of C–H bonds to an alcohol functionality, a reaction difficult to achieve by conventional methods of chemical synthesis [1]. This class of enzymes also catalyzes a wide variety of other reactions, including oxygen transfer to heteroatoms, epoxidation of olefins, hydroxylation of aromatic hydrocarbons and oxidative degradation of chemically inert xenobiotics such as drugs and environmental contaminants. The substrate range of P450 enzymes is very broad, ranging from simple alkanes to the most complex of hormones and their precursors [1]. This remarkable activity of cytochrome P450 arises from the highly activated transition metal complexes present in them. Many model systems based on transition metal complexes of porphyrins, phthalocyanines and Schiff bases that can mimic monooxygenase enzymes have been widely investigated [2]. The catalytic activity of the model complexes in homogeneous medium decreases with time due to ligand oxidation or formation of dimeric oxo- and peroxo-bridged complexes. Heterogenization of the homogeneous catalysts (metal complexes) has been sought to isolate the metal complexes to prevent their dimerization, increase their ruggedness and separability and to benefit from the synergistic catalytically beneficial interaction between the complexes and the support [3–8].

Heterogenization is achieved either by encapsulating the metal complex inside the pores of zeolites or by anchoring or tethering them to inert supports (figure 1)

[4]. Grafting and tethering refer to covalent attachment of the metal complex, either directly (grafting) or through a spacer ligand (tethering). The encapsulation (*ship-in-a-bottle*) approach is convenient and ideal because the complex, once formed inside the cages of the zeolite, is too large to diffuse out and is not lost into the liquid phase during the reaction. As these composite materials mimic biological enzymes, they are also called “zeozymes” (*acronym* for zeolite mimics of enzymes). On confinement in the zeolite matrix, the metal complex may lose some of its degrees of freedom and adopt unusual geometries that are stabilized by coordination to the zeolite-surface functional groups. In a general sense, the encapsulated complexes mimic enzyme systems in that the porous inorganic mantle (similar to the protein mantle in enzymes) provides (hopefully) the right steric requirement for the metal complex and imposes certain requirements (based on size and shape) to the access of the active site by the substrate molecules (substrate selectivity). Though many porous materials have been used, the most popular ones have been zeolites X and Y possessing large α -cages ($\sim 12 \text{ \AA}$ diameter).

Co(salen) complexes encapsulated in zeolite-Y were found to form more stable dioxygen adducts than the complexes in homogeneous solutions, mimicking hemoglobin [9]. In a similar attempt to prepare analogs of cytochrome P-450, Fe-phthalocyanine complexes were encapsulated in zeolite-Y, which exhibited remarkable substrate- and regio-selectivities in the oxidation of unactivated alkanes [10–14]. Jacobs and co-workers [10] reported a composite catalyst system that achieved realistic mimicry of cytochrome P-450 by incorporating Fe-phthalocyanine complex in the crystals of zeolite-Y, which were in turn embedded in a polydimethylsiloxane membrane. This system oxidized cyclohexane, at room

* To whom correspondence should be addressed.
E-mail: siva@cata.ncl.res.in

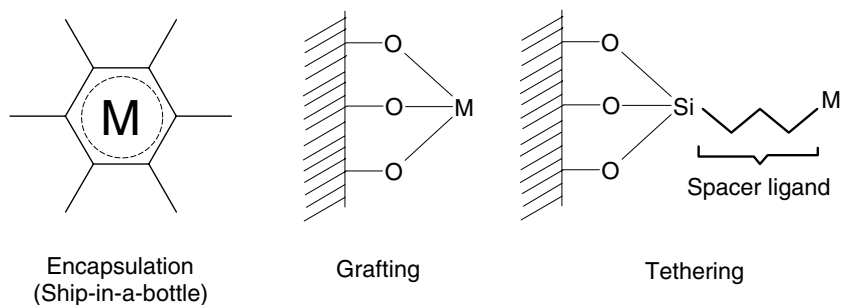


Figure 1. Methods of heterogenization of homogeneous catalysts (M = metal ion or complex).

temperature, at rates comparable to those of the enzymes.

Jacobs *et al.* have encapsulated Mn complexes of 2,2-bipyridine [15], 1,10-phenanthroline and triazacyclononane [16,17] in faujasite, HMS and MCM-41, as models for the methane monooxygenases. Mn porphyrin complexes embedded in polydimethylsiloxane (PDMS) exhibited high activity in the selective oxidation of cyclic alcohols to ketones with TBHP as the oxidant [18]. Copper amino acid complexes encapsulated in zeolite-Y catalyzed the oxidation of cyclohexane, benzyl alcohol, 1-pentanol and cyclohexene with TBHP as the oxidant [19]. Encapsulated Co(salophen) complexes were efficient O₂ activators in the Pd-catalyzed aerobic oxidation of 1,3-cyclohexadiene to 1,4 diacetoxy-2-cyclohexene [20–22]. Diegruber *et al.* [23] have reported the selective oxidation of propene to formaldehyde and acetone with dioxygen using Co(dm_g)₂-X and Co(py)-X catalysts. Oxidation of benzene to phenol using molecular oxygen as oxidant was also reported with these complexes.

Ogunwumi and Bein [24] and Sabater *et al.* [25] have investigated enantioselective epoxidation using encapsulated metal complexes. Piaggio *et al.* [26] have found that a Mn(III) chiral salen complex immobilized in Al-MCM-41 is an effective epoxidation catalyst for *cis*-stilbene.

In our laboratory, we have been working in the area of heterogenized homogeneous catalysts for more than a decade. This account reviews some of the results of this work. The systems reported are transition metal phthalocyanines, poly-aza macrocyclic complexes, Schiff bases, dimeric Cu-acetate and Co-Mn-carboxylate clusters encapsulated in zeolites and molecular sieves (figure 2(a) and (b)).

2. Metal phthalocyanines encapsulated in zeolites X and Y

An important aspect of encapsulation is to prove unequivocally the presence of metal complexes inside the cages (or cavities) of the zeolite. Though encapsulation is relatively easy with salen-type complexes, the problem is difficult in the case of phthalocyanines, which

are large in size (>12 Å diameter) and not easy to fit inside the zeolite cages, and which tend to adsorb strongly at the external surface of the crystallites. The encapsulation of copper, cobalt and vanadium phthalocyanines in the supercages (α -cages) of zeolite-Y (hitherto referred to as CuPcY, CoPcY and VPcY respectively) was carried out by the “*in situ* ligand synthesis method” using metal ion exchanged zeolite-Y and 1,2-dicyanobenzene [27]. The formation, integrity and location of MPc complexes in zeolite-Y were confirmed by elemental composition, surface area, thermogravimetric analysis (TG-DTA), FT-IR, UV-visible and EPR spectroscopic techniques [27–29].

Chemical composition and thermogravimetric analyses of CuPcY revealed the presence of 1.6 and 1.3 Pc molecules per unit cell when prepared from Cu-Y (Cu exchanged Y) containing 1.2 and 0.6% Cu respectively (table 1) [27]. Surface area (S_{BET}) and pore volume of zeolite-Y decreased after encapsulating the metal complexes (table 1). Phthalocyanine (Pc) exhibits characteristic π - π^* transitions (Q-bands) in the visible region 550–760 nm. The position and the number of these bands are highly sensitive to the geometry of the molecule. For the D_{4h} symmetry, Pc exhibits two Q-bands and for symmetry lower than D_{4h}, four Q-bands are observed. The positions of these bands for different samples are listed in table 2 [27]. The bands of CuPcY(0.6) and CuPcY(m) shifted to a lower energy (red shift), with the shift being more pronounced in the former (the band at 545 nm for the “neat” complex shifts to 581 nm for the encapsulated complex and to 574 nm for the physical mixture) (table 2). The red shift and the changes in relative intensities of the Q-bands are probably due to isolation of the molecules and puckering of the planar geometry of phthalocyanine due to encapsulation in zeolite-Y (figure 2b(i)). In H₂SO₄, the spectrum of CuPcY(0.6) and “neat” CuPc were similar confirming the formation and presence of CuPc in the encapsulated sample [27].

The EPR spectra of the encapsulated complexes (figure 3) indicate that the CuPc molecules are isolated and intermolecular interactions are negligible [27]. The encapsulated complexes show spectra with nine super-hyperfine features due to four equivalent nitrogens of the isoindole groups (resolution is clearer in the second

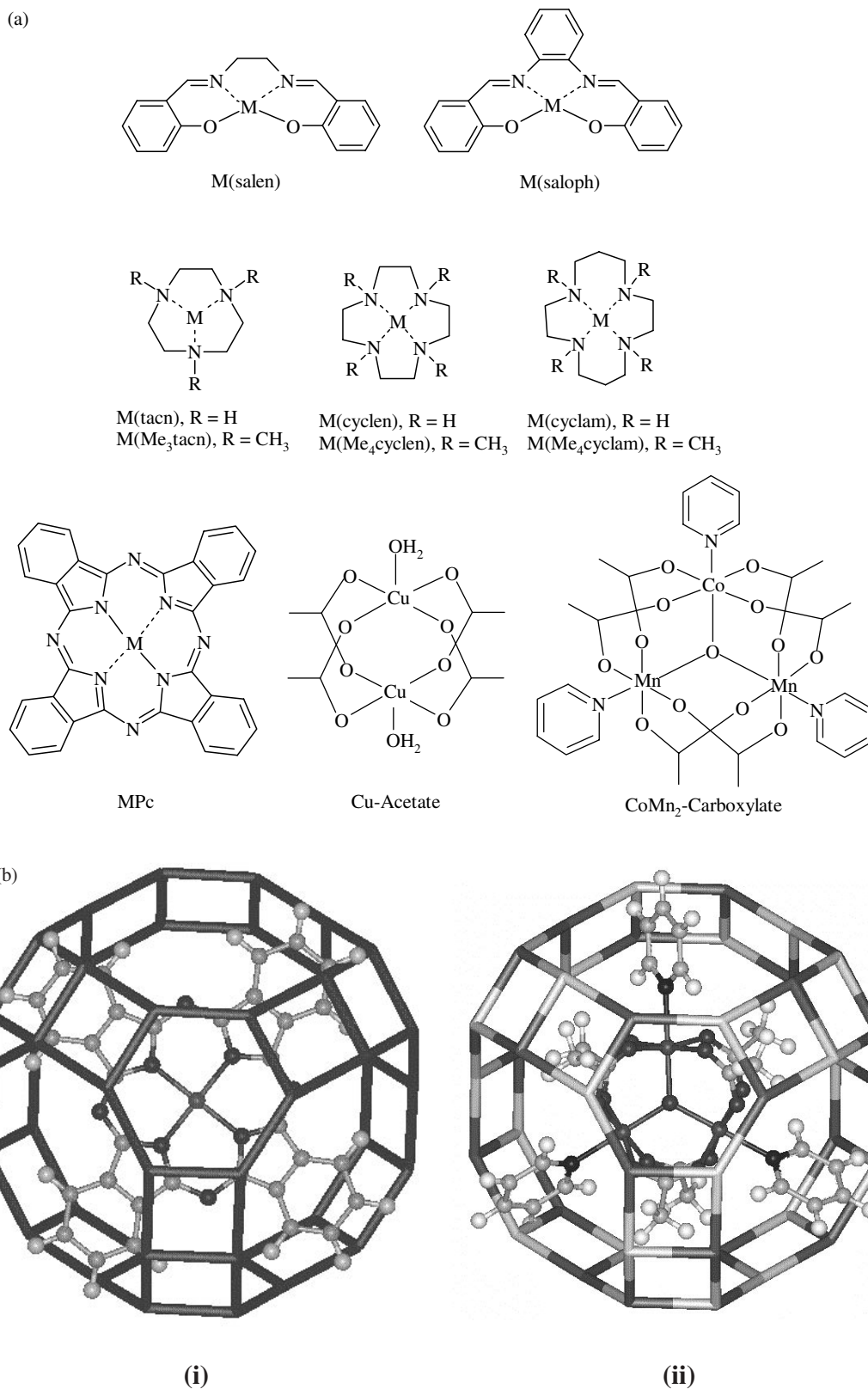


Figure 2. (a) Transition metal complexes used for encapsulation in zeolites and molecular sieves. (b) Molecular models of (i) metal phthalocyanine and (ii) Co-Mn-carboxylate-pyridine complexes in a supercage of zeolite-Y; the complexes are shown as ball and stick models.

Table 1
Chemical composition and textural characteristics of CuPcY

Sample	C/N analysis (wt.%)				Molecule/unit cell		S_{BET}^a (m ² /g)	Pore volume ^a (mL/g)
	Cu (wt.%)		C	N	Total Pc	CuPc		
	Total	As Pc						
CuPcY(1.2)	1.2	0.41	5.50	1.91	1.6	0.7	203	0.11
CuPcY(0.6)	0.6	0.46	4.68	1.74	1.3	0.8	573	0.22
CuY(1.2)	1.2	–	–	–	–	–	678	0.27

^aDegassing of sample done at 423 K and 10⁻⁵ mm prior to N₂ adsorption.

Table 2
Electronic spectral data of “neat” CuPc, CuPcY(0.6) and CuPcY(m)

Sample	Q-bands, nm
CuPc (neat)	545, 588, 686, 755
CuPcY(0.6)	581, 595, 706, 746
CuPc + NaY(mixture)	574, 592, 699, 755
CuPc in H ₂ SO ₄	702, 795
CuPcY(0.6) in H ₂ SO ₄	702, 795

derivative mode; figure 3). Hyperfine features due to copper are also resolved. The spectrum of the physical mixture does not show these hyperfine and super-hyperfine features (figure 3, trace c). Thus, EPR spectroscopy differentiates the CuPc molecules encapsulated in zeolites from those adsorbed at the surface of the crystallites. The spin Hamiltonian parameters ($g_{\parallel}=2.246$, $g_{\perp}=2.056$, $A_{\parallel}(\text{Cu})=189.5\text{G}$ and $A_{\perp}(\text{Cu})=14.2\text{G}$) indicate a tetragonally elongated square pyramidal geometry for copper and a puckering of the planar phthalocyanine moiety in the supercages.

Oxidation of styrene

Catalytic activities of CuPc in the “neat” state and when encapsulated in zeolite-Y were investigated at 333 K using TBHP as the oxidant. Styrene epoxide (–EPO), benzaldehyde (–CHO) and phenyl acetaldehyde (–CH₂CHO) were the major products. The encapsulated complexes exhibit higher activity than the “neat” complexes and the parent CuY (table 3) [27]. For example, CuPcY(1.2) gives a conversion of 94.2%, whereas the “neat” complex (4 mg; more than double the 1.8 mg of CuPc present in 0.05 g of CuPcY(1.2) used in the reaction) gives a conversion of 29.3%. Again, CuY(1.2) gives a conversion of 20.9%. After correcting for the anticipated conversion, due to the unreacted Cu present in CuPcY(1.2), a TON (turnover number) of 50.3 was obtained for encapsulated CuPc molecules [27]. The TON of CuPcY(0.6) is almost similar (table 3). Thus, the data suggest that activation of CuPc molecules occurs when they are encapsulated inside the supercages of zeolite-Y. A similar enhancement in the activity (by 2.8–3.2 times) was observed also with CoPc and VPc complexes [28]. The central metal ion had a pronounced effect on styrene conversion and product selectivity.

Styrene conversion increased in the order: V < Co < Cu. VPcY and CoPcY showed higher selectivity for styrene epoxide (–EPO), while CuPcY exhibited greater selectivity for benzaldehyde (–CHO) [28]. The enhanced activity of MPc complexes on encapsulation is probably a result of the distortion of the molecules (revealed by spectroscopic studies) and consequent ease of redox transformation of the metal ions.

Hydroxylation of phenol

Raja and Ratnasamy [29] have found high activity of copper phthalocyanine complexes (CuCl₁₄Pc and Cu(NO₂)₄Pc) encapsulated in zeolites X and Y in phenol hydroxylation. They prepared the samples by the “zeolite synthesis method” in which the complex is added to the synthesis gel during zeolite synthesis. While the chloro substituted complex yielded catechol (CAT) and hydroquinone (HQ) in a molar ratio of 1 : 1, the nitro-substituted Pc complexes yielded HQ as the only product. Thus, the above work reveals that peripheral substitution has a great effect on the product distribution in phenol hydroxylation [30]. Ramaswamy *et al.* [31] have immobilized CuCl₁₄Pc on alumina pillared montmorillonite using impregnation and ultrasonication methods and found that the catalysts prepared by the ultrasonication method are more active than those prepared by the impregnation method. The clay based catalysts exhibited moderate H₂O₂ selectivity (~30 mol%) with CAT/HQ (mol) = 1.1 and 1.4.

We have investigated the phenol hydroxylation activity of copper, cobalt and vanadium phthalocyanines encapsulated in zeolite-Y (prepared by the “ligand synthesis method”) (table 4) [29]. The activity at 12 h, for different catalysts varies in the order: CuPcY > CoPcY > VPcY. The difference in the performance of the catalysts arises because of differences in their relative activity in phenol hydroxylation and H₂O₂ decomposition. Additionally, differences in the location and accessibility of the different complexes, differences in the interaction with the zeolite framework and the presence of uncomplexed metal ions may also influence the performance of encapsulated MPc complexes. These catalysts prepared by the “*in situ* ligand synthesis method” are found to yield more CAT than HQ (table 4). The CAT/(HQ + PBQ) ratio is in the range 1.7 to 2 [29]. The complexes encapsulated by the “zeolite

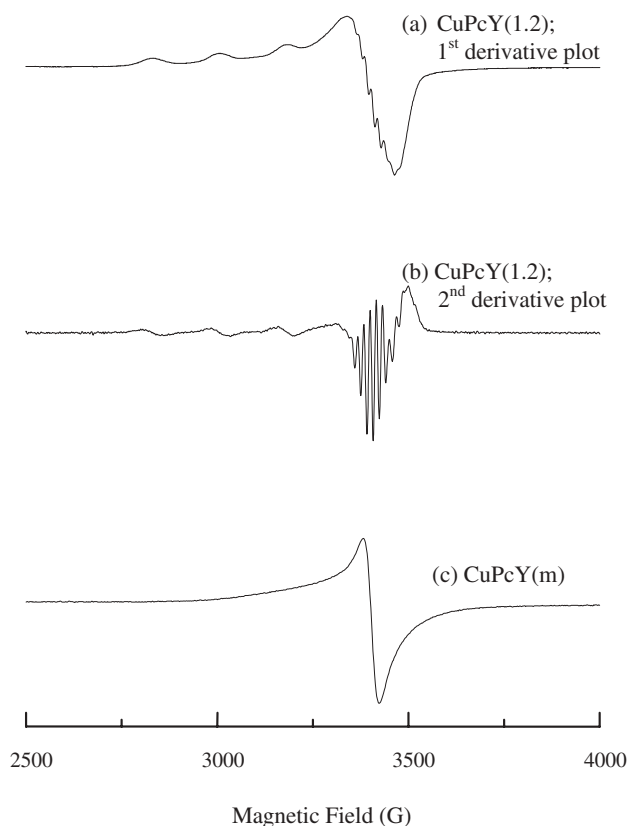


Figure 3. EPR spectra of (a) CuPcY(1.2)—in first derivative mode, (b) CuPcY(1.2)—in second derivative mode, and (c) CuPcY(m)—in first derivative mode at 298 K.

synthesis method” on the other hand yielded more HQ [30]. Thus, it appears that the method of encapsulation has a marked effect on phenol hydroxylation by MPcY complexes. Again, the catalysts prepared by the “*in situ* ligand synthesis method” exhibit larger TON (TON = 160–240) [29] compared to the catalysts prepared by the “zeolite synthesis method” (TON = 6–8) [30].

Other work carried out in our laboratory reveal that encapsulated phthalocyanines exhibit good activity in the C–H bond activation of *n*-alkanes [32,33] and cyclohexane [34]. Haloperoxidases are marine enzymes that oxyhalogenate aromatic substrates using H₂O₂ and halide ions present in the marine environment. Metal phthalocyanines encapsulated in zeolites X and Y exhibited haloperoxidase activity [35]. Oxychlorination and oxybromination of aromatics such as benzene, toluene, phenol, aniline, anisole and resorcinol were achieved at ambient conditions with H₂O₂/O₂ as the oxidant and HCl or alkali chloride or bromides as the sources of halogen [35].

3. Tri- and tetraaza macrocyclic complexes encapsulated in zeolite-Y

The manganese complexes of *N,N,N'*-trimethyl-1,4,7-triazacyclononane (Mn–Me₃tacn) exhibit remarkable catalytic activity in the presence of carboxylate

buffers, in the stereo-selective epoxidation of olefins, epoxidation of terminal and electron deficient olefins and oxidation of alkanes and alcohols, with H₂O₂, at ambient temperatures [36–38]. The activity of Mn–Me₃tacn depends on the nature of the carboxylate buffer, higher activity being observed in the presence of oxalate, ascorbate and citrate buffers than in the presence of acetate, malonate and tartrate buffers [39]. We found using FT-IR, UV-visible and EPR studies, the formation of terminal oxo and μ -oxo Mn species during the reaction. Their relative proportions varied with the carboxylate buffer and this was suggested by us to be the likely reason for the difference in the activity of Mn–Me₃tacn system in different carboxylate buffers [39]. We have also carried out studies on the encapsulation of tri- and tetraaza macrocyclic copper complexes (figure 2(a)). The structure of the encapsulated copper complexes and their activity in the C–H bond activation of ethylbenzene were investigated. The peraza macrocyclic complexes were encapsulated by the “flexible ligand synthesis method” by interacting copper exchanged NaY with the corresponding macrocyclic ligand [40].

The copper complexes of tacn and Me₃tacn were green while those of cyclen and Me₄cyclen were blue, and that of cyclam was red. The color of the complexes changed upon encapsulation in zeolite-Y. A systematic decrease in surface area (S_{BET}) with increasing molecular

Table 3
 Oxidation of styrene over CuPc complexes

Catalyst	Cu (exchange, wt%) ^a	Cu as CuPc (wt%)	Conversion (wt%)	TON ^b	Product distribution ^c			
					-CHO	-EPO	-CH ₂ CHO	Others
CuPcY(1.2)	0.79	0.41	94.2	50.3 ^d	43.5	39.1	13.7	3.8
CuPcY(0.6)	0.14	0.46	95.2	51.2 ^d	53.0	23.8	12.6	10.5
CuPc-“neat”	–	–	29.3	8.4 ^d	50.1	40.6	7.8	1.7
CuY	1.2	–	20.9	4.5 ^e	64.2	29.5	6.2	0.2

Note: Reaction conditions: styrene, 4.8 mmol; acetonitrile, 5 g; TBHP, 4.8 mmol; catalyst, 0.05 g (0.004 g in case of CuPc-“neat”); temperature, 333 K; reaction time, 24 h.

^aCu in exchange sites (uncomplexed with Pc).

^bTON = moles of styrene converted per mole of active component per hour.

^c-CHO = benzaldehyde, -EPO = styrene epoxide, -CH₂CHO = phenylacetaldehyde.

^dBased on CuPc.

^eBased on Cu ions in exchange positions.

dimensions of the ligand was observed. It was, however, noted that the changes in S_{BET} were smaller with the macrocyclic ligands (460–540 m²/g) compared to those observed for phthalocyanine complexes (203–678 m²/g). This is probably due to the smaller size of the cyclic peraza complexes (~5.5–8 Å) compared to the phthalocyanine complexes (>12 Å).

Figure 4 shows the UV-visible spectra of “neat” and zeolite-Y-encapsulated macrocyclic complexes. Acetonitrile solutions of the complexes reveal a characteristic UV band of ligand origin in the range, 250–300 nm. A weak band due to metal centered d–d transitions is observed in the visible range at 450–800 nm. A shift in the d–d band position from 660 nm (in tacn) to 505 nm (in cyclam) with an increase in the size of the macrocyclic ligand is noted. This shift in the band position to the higher energy side indicates that the tetraaza ligands (cyclam) provide higher stability. The ligand field is stronger in cyclam than in tacn complexes. The d–d band shifts to the higher energy side (15 nm in cyclam and 20 nm in tacn) when the complexes are encapsulated in zeolite-Y (figure 4b) suggesting a greater stability of the complexes on encapsulation inside the supercages of zeolite-Y.

Again, EPR spectroscopy has been used to provide convincing evidence for the formation and integrity of the complexes inside the supercages of zeolite-Y [40]. Cu(cyclam)²⁺ in CH₃CN shows a spectrum characteristic of axial symmetry. Hyperfine features due to copper are resolved in the parallel region. The spectrum of the encapsulated complex is almost similar to that of the frozen CH₃CN solution indicating the formation of molecules in zeolite supercages. Polycrystals of “neat” Cu(cyclam)²⁺ do not show such resolved copper hyperfine features due to intermolecular interactions that are avoided in frozen solutions and in encapsulated complexes. The similarity in the EPR spectrum of frozen solution and encapsulated Cu(cyclam)²⁺ complexes reveals that (as expected) the geometry of the complex did not change upon encapsulation (unlike the Pc complexes).

Oxidation of ethylbenzene

The peraza macrocyclic complexes exhibit good activity in the oxidation of ethylbenzene (table 5) [40]. The copper complexes of cyclen, Me₄cyclen and cyclam exhibit enhanced activities when they are encapsulated in zeolite-Y. The activity of Cu(tacn)²⁺ decreases upon

 Table 4
 Catalytic activity data of CuPcY, CoPcY and VPcY in phenol hydroxylation with H₂O₂

Catalyst	Phenol conversion (mol%)	TON ^a	H ₂ O ₂ efficiency (mol%) ^b	CAT/(HQ + PBQ) mol	Product distribution (mol%) ^c			
					PBQ	CAT	HQ	Others
CuPcY(0.6)	25.0	235	78.8	1.9	4.8	65.0	30.0	0.2
CuPcY(1.2)	26.5	203	85.0	1.6	6.4	62.0	31.2	0.3
CoPcY(0.6)	20.6	196	65.1	1.8	4.4	63.6	31.1	0.9
CoPcY(1.2)	17.4	168	57.0	1.7	8.1	62.7	28.2	1.1
VpcY(1.0)	19.8	242	67.6	2.0	6.3	62.0	24.2	7.5

Note: Reaction conditions: catalyst weight, 0.1 g; phenol: H₂O₂ (mol), 3; temperature, 348 K; solvent–water, 20 g; reaction time, 12 h.

^aTON = moles of phenol converted per mole of MPc.

^bH₂O₂ efficiency (%) = (moles of H₂O₂ consumed in products formation/moles of H₂O₂ taken × 100).

^cCAT = catechol, HQ = hydroquinone, PBQ = *para*-benzoquinone.

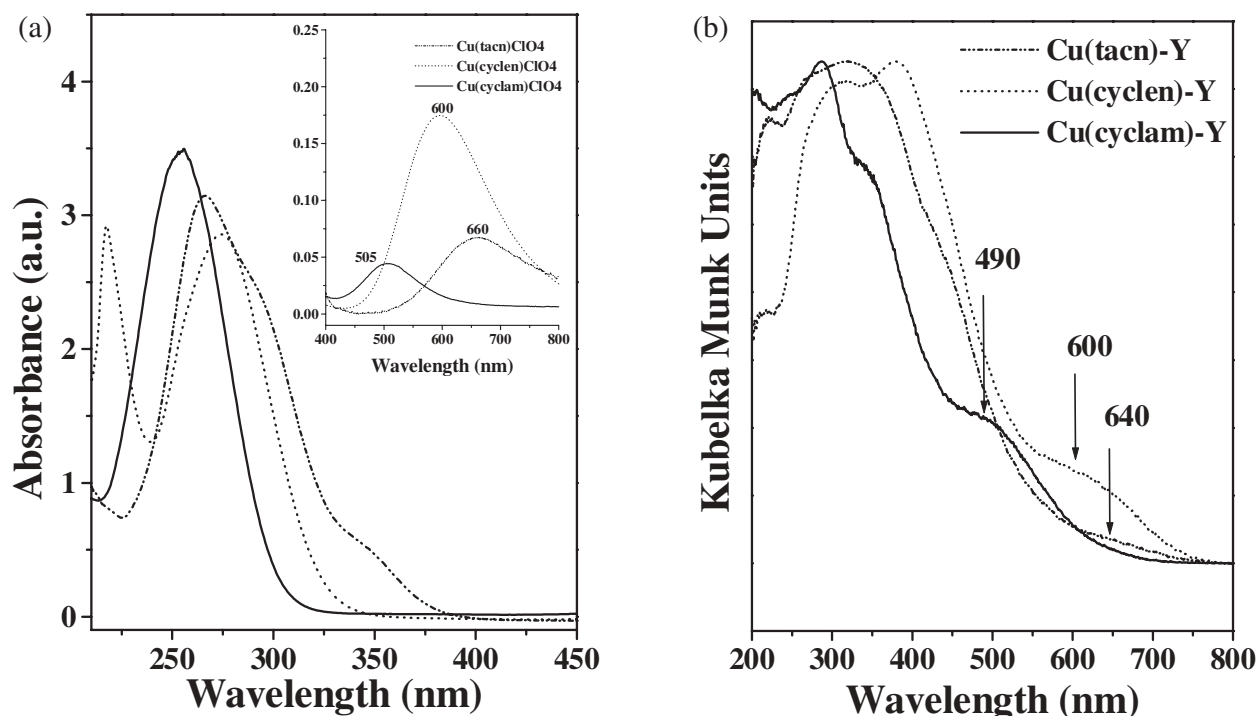


Figure 4. UV-visible spectra of “neat” (a) and encapsulated (b) Cu-tri and tetraaza macrocyclic complexes.

encapsulation. However, the encapsulated complexes exhibit enhanced selectivity for acetophenone (AcPh).

4. Metal Schiff base complexes encapsulated in zeolite-Y and adsorbed on Al-MCM-41

The Schiff base complexes of *N,N'*-ethylenebis(salicylidenediamine) (referred to as salen) and *N,N'*-*o*-phenylenebis(salicylidenediamine) (referred to as saloph) (figure 2(a)) are yet another group of metal complexes that have been widely studied as functional mimics of

metalloproteins in dioxygen binding and oxidation of olefins and aromatic compounds using H_2O_2 , iodosylbenzene, NaOCl , etc. [41–47]. The Schiff base complexes are conformationally flexible and adopt a variety of geometries, viz. planar, umbrella-type and stepped conformations, to generate various active site environments for the different oxidation reactions. This flexibility, similar to that observed in metalloproteins, is the key factor for the biomimetic activity of these molecules. $\text{Cu}(\text{salen})$ complexes were encapsulated in zeolites X and Y by the “flexible ligand synthesis method” by interacting $\text{Cu}(\text{II})$ exchanged zeolite-Y with

Table 5
Oxidation of ethylbenzene using tetraaza $\text{Cu}(\text{II})$ complexes

Catalyst	Time (h)	Conv. mol%	TOF ^a	Selectivity (%)			
				AcPh	<i>o</i> -hydroxy AcPH	<i>p</i> -hydroxy AcPH	Others
$\text{Cu}(\text{tacn})(\text{ClO}_4)_2$	10	49.6	24.8	91.0	1.1	2.6	5.3
$\text{Cu}(\text{tacn})\text{-Y}$	10	37.0	19.8	97.0	–	2.9	0.1
$\text{Cu}(\text{cyclen})(\text{ClO}_4)_2$	8	19.0	6.0	64.2	7.0	1.0	27.8
$\text{Cu}(\text{cyclen})\text{-Y}$	10	30.5	12.6	80.2	–	4.3	15.5
$\text{Cu}(\text{Me}_4\text{cyclen})(\text{ClO}_4)_2$	10	35.1	8.8	71.0	3.8	9.7	15.5
$\text{Cu}(\text{Me}_4\text{cyclen})\text{-Y}$	10	27.8	11.2	85.9	–	6.3	7.8
$\text{Cu}(\text{cyclam})(\text{ClO}_4)_2$	10	44.5	11.1	85.9	4.9	2.9	6.3
$\text{Cu}(\text{cyclam})\text{-Y}$	10	44.4	17.1	98.0	–	2.0	–

Note: Reaction conditions: substrate, 0.106 g (1 mmol); catalyst, 0.2 mol% of substrate (in case of “neat” catalysts) and 0.02 g (in case of encapsulated catalysts); TBHP (50% in ethylene dichloride), 0.3 mL; solvent, CH_3CN (1 mL); temperature, 333 K; reaction time, 10 h.

^aTOF = moles of ethylbenzene converted per mole of catalyst per hour; AcPh = acetophenone.

Table 6
Catalytic activity of “neat” and zeolite-encapsulated substituted Cu(salen) complexes

Catalyst	Catalytic activity				
	<i>Para</i> -xylene oxidation conversion (wt%) ^a	Phenol oxidation ^b		TBHP decomposition TOF ^{c,e}	H ₂ O ₂ decomposition TOF ^{d,e}
		Conversion (wt%)	TOF ^c		
Cu(salen)	3.4	6.2	21	53	36
Cu(salen)-Y	45.1	5.4	40	1704	2 32 506
Cu(5-Cl-salen)	4.6	7.7	31	108	64
Cu(5-Cl-salen)-Y	48.9	6.8	88	29 377	4 54 949

^aReaction conditions for *para*-xylene oxidation: *para*-xylene, 30 g; solid catalyst, 0.5 g; TBHP, 0.5 g; oxidant, air (33 bar); temperature, 403 K; reaction time, 18 h.

^bReaction conditions for phenol oxidation: phenol, 4.7 g; solid catalyst, 0.05 g; aqueous H₂O₂ (30%), 1.13 g; temperature, 353; reaction time, 1 h.

^cReaction conditions for TBHP decomposition: catalyst, 0.025 g; TBHP, 5 g; temperature, 298 K; reaction time, 1 h.

^dReaction conditions for H₂O₂ decomposition: catalyst, 0.025 g; aqueous H₂O₂ (30%), 5.5 g; temperature, 298 K; reaction time, 1 h.

^eTOF = moles of substrate converted per mole of Cu per hour.

salen ligand. The catalytic activity was investigated for *p*-xylene and phenol oxidations and for the decomposition of H₂O₂ and TBHP [45]. In all the cases, the intrinsic catalytic activity of Cu(salen) complexes enhanced significantly on encapsulation in zeolites (table 6). The activity was higher with electron withdrawing Cl substitution in the ligand (table 6). EPR spectroscopy and other physicochemical techniques have revealed changes in the geometry of salen complexes on encapsulation [45]. The hyperfine coupling parameters and covalency parameter (estimated from EPR spin Hamiltonian values) indicated a greater depletion of electron density at the site of Cu when the molecules were encapsulated. This depletion in turn facilitated the nucleophilic attack by reagents like TBHP anion at the metal center. Since transition metal hydroperoxides are known oxidation catalysts, an enhancement in their rates of formation will increase the catalytic activity. This is in agreement with the catalytic activity data presented in table 6. The Cu(II)/Cu(I) redox couple appeared at less negative potentials for Cu(5-Cl-salen) than for Cu(salen). The EPR studies revealed that the encapsulated complexes are present in

a distorted tetrahedral conformation [45]. A tetrahedral distortion of the square planar complex will increase the Cu(II)/Cu(I) reduction potential leading to a further enhancement of the oxidation reaction. It was revealed that the copper ions or complexes leached out of the zeolite during the reaction, if any, do not make a significant contribution to the observed catalytic activity. In fact, the significant enhancement (by orders of magnitude) in the intrinsic catalytic activity (turnover frequencies) of the zeolite-encapsulated salens *vis-à-vis* the “neat” complexes is a strong indication that it is the catalytic behavior of the isolated copper salens inside the cavities of the zeolite that is responsible for the observed enhancement in the catalytic activity [45].

Vanadium saloph complexes (VO(saloph)) exhibited similar enhancement in the activity (by 3 to 5 times) and selectivity in styrene and *trans*-stilbene epoxidations with TBHP when they were encapsulated in zeolite-Y and Al-MCM-41 by the “flexible ligand synthesis method” contacting saloph and vanadium exchanged NaY and Al-MCM-41 molecular sieves respectively (table 7) [47]. VO(saloph) encapsulated in Al-MCM-41 is relatively more active than that encapsulated in

Table 7
Epoxidation of *trans*-stilbene and styrene by “neat” and zeolite-Y and Al-MCM-41-encapsulated VO(saloph) complexes

Catalyst (wt, mg)	<i>Trans</i> -stilbene epoxidation			Styrene epoxidation				
	Conv. (wt%)	TOF ^a	Epoxide (wt%)	Conv. (wt%)	TOF ^a	Product selectivity (wt%)		
						-CHO	Epoxide	Others
VO(saloph) (5)	9.3	256	73.4	10.7	726	32.3	9.4	58.3
VO(saloph)-Y (50)	36.8	1013	84.8	34.8	2362	11.5	35.5	53.0
VO(saloph)-Al-MCM-41 (20)	48.1	1324	88.5	40.6	2753	7.7	45.0	47.3

Note: Reaction conditions: *trans*-stilbene epoxidation: *trans*-stilbene, 1.8 g (10 mmol); CH₃CN, 15 g; TBHP, 2.56 g (20 mmol); temperature, 363 K; run time, 5 h. Styrene epoxidation: styrene, 1.04 g (10 mmol); CH₃CN, 20 g; TBHP, 2.56 g (20 mmol); temp, 363 K; run time, 2 h.

^aTOF = moles of substrate converted per mole of vanadium per hour.

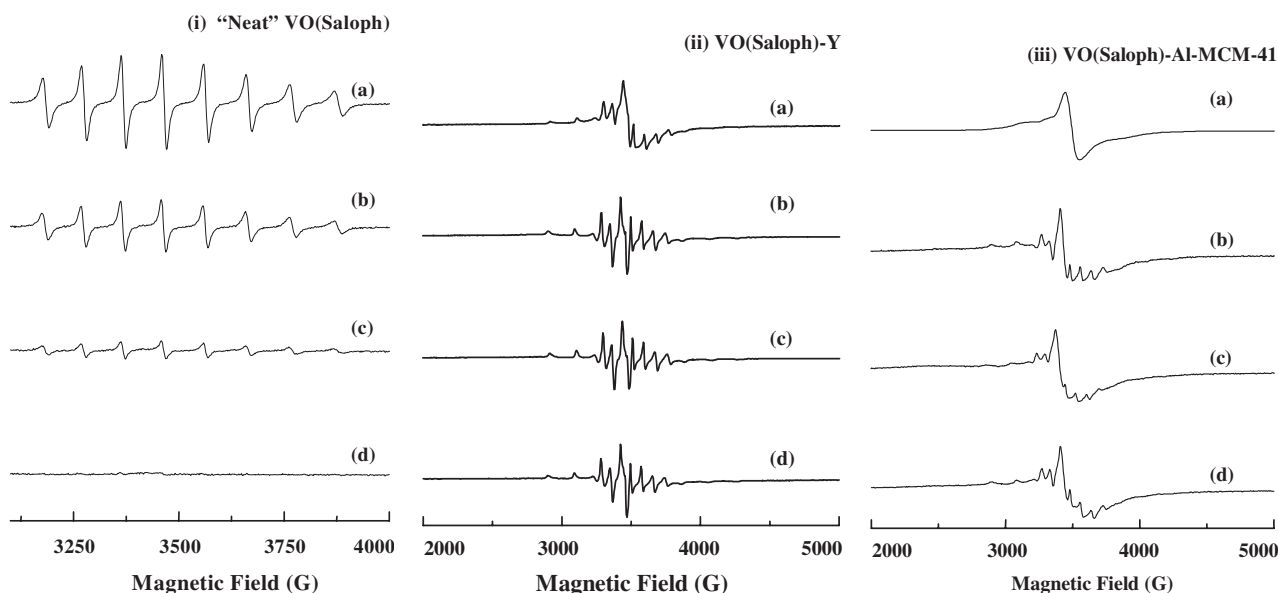


Figure 5. EPR spectra of the catalysts at 298 K during *trans*-stilbene oxidation: (i) “neat” VO(saloph), reaction time—(a) 0, (b) 30, (c) 60 and (d) 135 min; (ii) VO(saloph)-Y, reaction time—(a) 0, (b) 2, (c) 4 and (d) 6–24 h; (iii) VO(saloph)-Al-MCM-41, reaction time—(a) 0, (b) 2, (c) 4 and (d) 6–24 h.

zeolite-Y. EPR studies revealed that upon encapsulation inside the pores of Al-MCM-41, the structure of VO(saloph) changes from square pyramidal to an octahedral geometry. The relaxed geometry of VO(saloph) and easy access of the active site to the substrate molecules are perhaps the causes for the higher activity of VO(saloph) located in Al-MCM-41. *In situ* EPR spectroscopy was used to obtain evidence that the complexes are active throughout the reaction and leaching of metal ions into the solution was minimal in encapsulated complexes [47]. For the *in situ* experiments, in the reaction with “neat” VO(saloph), a known quantity of the reaction mixture was taken out at different time intervals and subjected to the spectroscopic studies. In the case of encapsulated catalysts, the reactions were performed for a specific period of time and then the catalyst was separated, dried and characterized by EPR. Representative spectra of “neat” and encapsulated VO(saloph) as a function of reaction time are shown in figure 5. For the reactions in a homogeneous medium, the intensity of the vanadium EPR signals decreased with time and disappeared at 135 min (figure

5(i), trace d). In the absence of substrate, (*trans*-stilbene) the signals disappeared at 105 min itself. Interestingly, the encapsulated catalysts were EPR active even after 24 h (figures 5(ii) and (iii); trace d). VO(saloph) forms vanadium peroxo complexes on interaction with TBHP. The peroxo complex transfers one of its oxygen atoms to the substrate and transforms into an oxo-hydroxo or dioxo-vanadium species. In the homogeneous medium, these species react further to form EPR inactive μ -oxo-vanadium(IV) complexes. The latter are catalytically inactive. However, in the solid catalysts, VO(saloph) molecules are well separated owing to confinement in the cages or interactions with the support (as revealed by EPR) and they remain active throughout the reaction (figures 5(ii) and (iii); trace d) [47].

5. Dimeric copper acetate complexes encapsulated in zeolite-Y

In an attempt to activate dioxygen to mimic the oxygenase activity of metalloenzymes, copper acetate

Table 8
Hydroxylation of phenol using molecular oxygen

Catalyst	Phenol conv. (mol%)	TOF ^a	<i>o</i> -Benzoquinone (mol%)	Others (mol%)
Cu acetate-“neat”	5.1	3.6	4.9	0.2
Cu acetate-Y	11.5	60.9	11.5	–
Cu chloroacetate-“neat”	1.0	0.9	1.0	–
Cu chloroacetate-Y	12.0	227.1	11.9	0.1

Note: Reaction conditions: phenol, 1.88 g; catalyst, 0.073 g; phosphoric acid buffer (pH = 6.5), 20 mL; oxygen, 1 atm; temperature, 298 K; reaction time, 19 h.

^aTOF = moles of phenol converted per mole of Cu per hour.

Table 9
Catalytic activity of μ_3 -oxo metal cluster complexes in selective oxidation of *p*-xylene

Catalyst	Run time (h)	Conv. wt%	Product distribution (wt%)					
			<i>p</i> -Tolyl alcohol	<i>p</i> -Tolu-aldehyde	<i>p</i> -Toluic acid	4-Carboxy benzaldehyde	Terephthalic acid	Benzoic acid
Co ₃ (O)	2	73.1	0.7	32.4	20.4	28.9	16.6	1.0
Mn ₃ (O)	2	77.0	–	35.8	8.6	1.6	53.8	0.2
CoMn ₂ (O)	2	100.0	–	–	1.8	0.4	97.8	–
Co ₃ (O)-Y	4	69.9	–	28.4	49.5	7.7	12.7	1.7
Mn ₃ (O)-Y	4	99.9	–	–	20.1	0.7	79.2	–
CoMn ₂ (O)-Y	4	100.0	–	–	0.6	0.01	99.4	–

Note: Reaction conditions: catalyst, 0.0342 g (neat complex) or 0.2995 g (encapsulated catalyst), *p*-xylene, 2 mL; NaBr, 0.0865 g; water, 5.6 mL; acetic acid, 38 mL; air, 550 psig; temperature, 473 K).

dimers (figure 2(a)) were encapsulated in molecular sieves Y, MCM-22 and VPI-5 by treating the copper exchanged zeolites with acetic acid vapors [48–50]. The complexes regioselectively *ortho*-hydroxylated L-tyrosine to L-DOPA, phenol to catechol and *ortho*-benzoquinone and cresols to the corresponding *ortho*-dihydroxy and *ortho*-quinone compounds [48–50]. This zeozyme, hence, functionally mimics the copper monooxygenase, tyrosinase. The latter employs a coupled dicopper site to *ortho*-hydroxylate monophenols and converts the resulting catechols to *ortho*-quinones. The encapsulated complexes exhibited enhanced activities compared to the “neat” copper acetate in homogeneous medium [48–50]. Chloroacetato complexes of copper showed still higher activities [50]. Representative data on the hydroxylation of phenol are presented in table 8. The structure activity correlations for the enhanced activity of copper acetate and chloroacetate were investigated using several physicochemical techniques including variable temperature EPR [50]. The studies revealed that there are significant differences in the properties of “neat” and encapsulated complexes. On encapsulation in the zeolite, the Cu–Cu exchange coupling constant, $-J$, increases to 310 from 250 cm⁻¹ for the “neat” complex (i.e., by about 19.7%). Simultaneously, the Cu–Cu separation in the dimer, estimated indirectly from the exchange coupling constant, shortens to 2.40 Å in the encapsulated state from 2.64 Å in the “neat” copper acetate complex. There is, hence, a relatively greater overlap of the metal orbitals of the dimer copper atoms inside the restricted confines of the zeolite cages. The consequent, enhanced, *trans*-axial lability of the phenolate and dioxygen ligands promotes the catalytic oxygenase activity of copper acetate and chloroacetate dimers on encapsulation in zeolites.

6. Co-Mn-carboxylate complexes encapsulated in Zeolite-Y

Trinuclear μ_3 -oxo mixed metal acetato complexes, [CoMn₂(μ_3 -O)(CH₃COO)₆(pyridine)₃] encapsulated in

zeolite-Y (referred as CoMn₂(O)-Y; figure 2b(ii)) exhibited high catalytic efficiency in the selective aerial oxidation of *p*-xylene to terephthalic acid [51,52]. Interestingly, the formation of 4-carboxybenzaldehyde, the worrisome impurity in the conventional process, was suppressed significantly over these solid catalysts [51,52]. The presence of 4-carboxybenzaldehyde imparts color to the terephthalic acid product and its concentration is reduced conventionally, at great cost, by a post-oxidation-hydrogenation process. Terephthalic acid, one of the largest volume commodity chemicals, is commercially manufactured by dioxygen oxidation of *p*-xylene using cobalt and manganese salts, at 473–500 K, in acetic acid solvent and bromide ion as promoter [53]. On the basis of detailed *in situ* spectroscopic studies, we have found that reactive μ_3 -oxo Co/Mn mixed clusters are formed in the homogeneous reaction medium [54]. This finding was substantiated by preparing the oxo clusters externally and evaluating their catalytic activity. These complexes were then encapsulated inside the supercages of zeolite-Y using the “flexible ligand synthesis method” [51,52]. Studies were performed also on the homonuclear clustered Co and Mn complexes (Co₃(O) and Mn₃(O), respectively). Catalytic activities of these cluster complexes in “neat” form and when encapsulated in zeolite-Y are reported in table 9. The solid heterogeneous catalyst, CoMn₂(O)-Y, at 100% conversion of *p*-xylene, was even more selective (99.4% selectivity for terephthalic acid; only 0.01% of 4-carboxybenzaldehyde) than the “neat” cluster and conventional homogeneous catalysts. With encapsulated complexes, a longer reaction time (4 h) was required for complete conversion of *para*-xylene [52]. The “neat” and conventional catalysts required only 2 h. This is probably due to diffusional limitations in the zeolite catalysts. The solid catalysts were separated by simple filtration from the terephthalic acid by converting the latter into a water-soluble sodium salt. The separated catalyst had similar activity (on recycle) and spectroscopic characteristics as that of the fresh catalyst indicating the preservation of its structural integrity and reusability. Only a trace amount of metal ions (0.5% of

the metal in the zeolite; about 50 ppm of Mn in solution) leached into the reaction medium, which is too low to account for the observed catalytic activity. To our knowledge, this is the first example of the use of a solid catalyst for the oxidation of *p*-xylene to terephthalic acid with catalytic efficiencies comparable, if not superior, to that of the state-of-the-art homogeneous catalyst. The heteronuclear Co–Mn carboxylato clusters also exhibited efficient activity in the oxidation of cyclohexane, cyclohexanol and cyclohexanone to adipic acid, yet another commercially important transformation [55].

7. Conclusions

A variety of transition metal complexes of phthalocyanines, tri- and tetraaza macrocycles, Schiff bases (salen and saloph) and acetates were encapsulated inside the pores and cages of zeolites and molecular sieves. Biomimetic activity of the encapsulated complexes in the selective oxidation of a variety of important organic transformations (e.g., oxyfunctionalization of hydrocarbons, hydroxylation of phenol, epoxidation of styrene, oxidation of *p*-xylene to terephthalic acid and oxidation of cyclohexane, cyclohexanol and cyclohexanone to adipic acid) was investigated. The encapsulated complexes were found to be superior to the corresponding “neat” complexes. Enhanced activity, and in some cases improved selectivity, were obtained using the encapsulated complexes. The possible reasons for the enhanced activity of different encapsulated complexes were investigated using spectroscopic (especially EPR and UV-visible) methods. These were identified as (i) isolation of individual molecules and distortion of molecular geometry from planarity to a “puckered” structure in metal phthalocyanines; (ii) synergism of the encapsulated complexes and the zeolite framework in peraza macrocycles; (iii) a greater depletion of electron density at the site of metal ion facilitating nucleophilic attack by reagents like TBHP anion at the metal center in Schiff base complexes; (iv) shortening of Cu–Cu distance, greater overlap of metal orbitals and the consequent *trans*-axial lability of metal–oxygen and metal–substrate bonds in dimeric Cu–acetates; and (v) synergism of Co, Mn and zeolite interactions facilitating the ease of Co(III)/Co(II) and Mn(II)/Mn(III) redox couples in the case of Co–Mn–acetate complexes. The study reveals that encapsulated metal complexes can truly mimic the functionality of metalloenzymes, thus providing scope for future applications.

References

- [1] H.A.O. Hill, P.J. Sadler and A.J. Thomson (eds), *Metal Sites in Proteins and Models: Iron Centers, Structure & Bonding*, Vol. 88 (Springer-Verlag, Berlin, 1997).
- [2] R.D. Jones, D.A. Summerville and F. Basolo, *Chem. Rev.* 79 (139) 1979.
- [3] N. Herron, *CHEMTECH* 19 (1989) 542.
- [4] K.J. Balkus Jr. and A.G. Gabrielov, *J. Incl. Phenom. Mol. Recog. Chem.* 21 (1995) 159.
- [5] J.J.E. Moreau and M.W.C. Man, *Coord. Chem. Rev.* 178–180 (1998) 1073.
- [6] D. Brunel, N. Bellocq, P. Sutra, A. Cauvel, M. Lasperas, P. Moreau, F. Di Renzo, A. Galarneau and F. Fajula, *Coord. Chem. Rev.* 178–180 (1998) 1085.
- [7] A. Choplin and F. Quignard, *Coord. Chem. Rev.* 178–180 (1998) 1679.
- [8] D.E. De Vos, M. Dams, B.F. Sels and P.A. Jacobs, *Chem. Rev.* 102 (2002) 3615.
- [9] N. Herron, *Inorg. Chem.* 25 (1986) 4714.
- [10] R.F. Parton, I. Vankelecom, C.P. Bezoukhanova, M. Casselman, J. Uytterhoeven and P.A. Jacobs, *Nature* 370 (1994) 541.
- [11] R.F. Parton, C.P. Bezoukhanova, F. Thibault-Starzyk, R.A. Raynders, P.J. Grobet and P.A. Jacobs, *Stud. Surf. Sci. Catal.* 84 (1994) 813.
- [12] R.F. Parton, C.P. Bezoukhanova, J. Grobet, P.J. Grobet and P.A. Jacobs, *Stud. Surf. Sci. Catal.* 83 (1994) 371.
- [13] K.J. Balkus Jr., M. Eissa and R. Lavado, *J. Am. Chem. Soc.* 117 (1995) 10753.
- [14] E. Armengol, A. Corma, V. Fornes, H. Garcia and J. Primo, *Appl. Catal. A: Gen.* 181 (1999) 305.
- [15] P.P. Knops-Gerrits, D.E. De Vos, F. Thibault-Starzyk and P.A. Jacobs, *Nature* 369 (1994) 543.
- [16] D.E. De Vos, S. De Wildeman, B.F. Sels, P.J. Grobet and P.A. Jacobs, *Angew. Chem. Int. Ed. Engl.* 38 (1999) 1033.
- [17] Y.V.S. Rao, D.E. De Vos, T. Bein and P.A. Jacobs, *Chem. Commun.* (1997) 355.
- [18] P.E.F. Neys, I.F.J. Vankelecom, R.F. Parton, W. Dhaen, G. L’abbe and P.A. Jacobs, *J. Mol. Catal. A: Chem.* 126 (1997) L9.
- [19] B.P. Murphy, *Coord. Chem. Rev.* 124 (1993) 63.
- [20] J. Woltinger, J.E. Backvall and A. Zsigmond, *Chem. Eur. J.* 5 (1999) 1460.
- [21] A. Zsigmond, F. Notheisz, Z. Frater and J.E. Backvall, *Stud. Surf. Sci. Catal.* 108 (1997) 453.
- [22] A. Zsigmond, F. Notheisz, Z. Szegletes and J.E. Backvall, *Stud. Surf. Sci. Catal.* 94 (1995) 728.
- [23] H. Diegrubber, P.J. Plath and G. Schulz-Ekloff, *J. Mol. Catal.* 24 (1984) 115.
- [24] S.B. Ogunwumi and T. Bein, *Chem. Commun.* (1997) 901.
- [25] M.J. Sabater, A. Corma, A. Domenech, V. Fornes and H. Garcia, *Chem. Commun.* (1997) 1285.
- [26] P. Piaggio, P. McMorn, C. Langham, D. Bethell, P.C. Bulman-Page, F.E. Hancock and G.J. Hutchings, *New J. Chem.* (1998) 1167.
- [27] S. Seelan, A.K. Sinha, D. Srinivas and S. Sivasanker, *J. Mol. Catal. A: Chem.* 157 (2000) 163.
- [28] S. Seelan, D. Srinivas, M.S. Agashe, N.E. Jacob and S. Sivasanker, *Stud. Surf. Sci. Catal.* 135 (2001) 2224.
- [29] S. Seelan, A.K. Sinha, D. Srinivas and S. Sivasanker, *Bull. Catal. Soc. India* 1 (2002) 29.
- [30] R. Raja and P. Ratnasamy, *Stud. Surf. Sci. Catal.* 101 (1996) 181.
- [31] V. Ramaswamy, M. Sivarama Krishnan, A.V. Ramaswamy, *J. Mol. Catal., A: Chem.* 181 (2002) 81.
- [32] R. Raja and P. Ratnasamy, *Appl. Catal., A: Gen.* 158 (1997) L7.
- [33] R. Raja, C.R. Jacob and P. Ratnasamy, *Catal. Today* 49 (1999) 171.
- [34] R. Raja and P. Ratnasamy, *Catal. Lett.* 48 (1997) 1.
- [35] R. Raja and P. Ratnasamy, *J. Catal.* 170 (1997) 244.
- [36] D.E. De Vos, B.F. Sels, M. Reynaers, Y.V. Subba Rao and P.A. Jacobs, *Tetrahedron Lett.* 39 (1998) 3221.
- [37] J.R.L. Smith and G.B. Shul’pin, *Tetrahedron Lett.* 39 (1998) 4909.

- [38] G.B. Shul'pin, G. Suss-Fink and L.S. Shul'pin, *J. Mol. Catal. A: Chem.* 170 (2001) 17.
- [39] T.H. Bennur, S. Sabne, S.S. Deshpande, D. Srinivas and S. Sivasanker, *J. Mol. Catal. A: Chem.* 185 (2002) 71.
- [40] T.H. Bennur, D. Srinivas and S. Sivasanker, unpublished results.
- [41] S.P. Varkey, C. Ratnasamy and P. Ratnasamy, *J. Mol. Catal. A: Chem.* 135 (1998) 295.
- [42] C.R. Jacob, S.P. Varkey and P. Ratnasamy, *Appl. Catal. A: Gen.* 168 (1998) 353.
- [43] C.R. Jacob, S.P. Varkey and P. Ratnasamy, *Appl. Catal. A: Gen.* 182 (1999) 91.
- [44] C.R. Chandra, S.P. Varkey and P. Ratnasamy, *Microporous Mesoporous Mater.* 22 (1998) 465.
- [45] S. Deshpande, D. Srinivas and P. Ratnasamy, *J. Catal.* 188 (1999) 261.
- [46] T.H. Bennur, D. Srinivas and P. Ratnasamy, *Microporous Mesoporous Mater.* 48 (2001) 111.
- [47] T. Joseph, D. Srinivas, C.S. Gopinath and S.B. Halligudi, *Catal. Lett.* 83 (2002) 209.
- [48] R. Robert and P. Ratnasamy, *J. Mol. Catal. A: Chem.* 100 (1995) 93.
- [49] S.A. Chavan, D. Srinivas and P. Ratnasamy, *Top. Catal.* 11/12 (2000) 359.
- [50] S.A. Chavan, D. Srinivas and P. Ratnasamy, *J. Catal.* 192 (2000) 286.
- [51] S.A. Chavan, D. Srinivas and P. Ratnasamy, *Chem. Commun.* (2001) 1124.
- [52] S.A. Chavan, D. Srinivas and P. Ratnasamy, *J. Catal.* 204 (2001) 409.
- [53] W. Partenheimer, *Catal. Today* 23 (1995) 69.
- [54] S.A. Chavan, S.B. Halligudi, D. Srinivas and P. Ratnasamy, *J. Mol. Catal. A: Chem.* 161 (2000) 49.
- [55] S.A. Chavan, D. Srinivas and P. Ratnasamy, *J. Catal.* 212 (2002) 39.